Journal Pre-proof

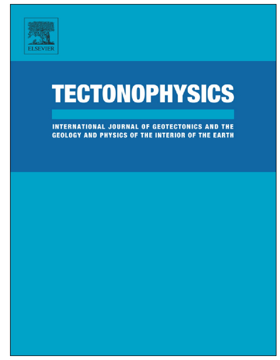

Gravimetric survey and modelling of a tectonic indenter boundary: The Palomares Fault Zone (Betic Cordillera, Iberia)

V. Tendero-Salmerón, G. Ercilla, L. González-Castillo, A. Madarieta-Txurruka, F.J. Martínez-Moreno, F. Estrada, J. Galindo-Zaldivar

PII: S0040-1951(23)00445-6

DOI: https://doi.org/10.1016/j.tecto.2023.230147

Reference: TECTO 230147

To appear in: *Tectonophysics*

Received date: 13 October 2022

Revised date: 12 November 2023

Accepted date: 17 November 2023

Please cite this article as: V. Tendero-Salmerón, G. Ercilla, L. González-Castillo, et al., Gravimetric survey and modelling of a tectonic indenter boundary: The Palomares Fault Zone (Betic Cordillera, Iberia), *Tectonophysics* (2023), https://doi.org/10.1016/j.tecto.2023.230147

Gravimetric survey and modelling of a tectonic indenter boundary: The Palomares Fault Zone (Betic Cordillera, Iberia)

Tendero-Salmerón, V.[1,3]*, Ercilla, G.[2], González-Castillo, L.[3], Madarieta-Txurruka, A.[3], Martínez-Moreno, F.J.[4], Estrada, F.[2], Galindo-Zaldivar, J.[1,3]

[1]Instituto Andaluz de Ciencias de la Tierra (CSIC-UGR), 18100 Armilla (Granada), Spain

[2]Instituto de Ciencias del Mar, CSIC, Continental Margins Group, 08003 Barcelona, Spain

[3]Departamento de Geodinámica, Universidad de Granada, 18071 Granada, Spain

[4]Departamento de Geodinámica, Paleontología y Estratigrafía, Universidad Complutense de Madrid, 28040 Madrid, Spain.

***Corresponding author:** Víctor Tendero Salmerón – vtendero@ugr.es

E-mail addresses: vtendero@ugr.es (V. Tendero-Salmerón), gemma@icm.csic.es (G. Ercilla), lgcastillo@ugr.es (L. González-Castillo), amadatxu@ugr.es (A. Madarieta-Txurruka), fjmmoreno@ucm.es (F. J. Martínez-Moreno), festrada@icm.csic.es (F. Estrada), jgalindo@ugr.es (J. Galindo-Zaldivar)

Abstract

New gravimetric data are improving our understanding of the Palomares Fault Zone (PFZ) that accommodates the Águilas Arc tectonic indentation (eastern Betic Cordillera, SE Iberia) in the context of the Eurasia-Africa convergence. The PFZ limits the sedimentary infill geometry of the Vera and Pulpí Basins, and the western Guadalentín Corridor, which are located along the western boundary of the arc. Gravity anomaly models are in agreement with previous tectonic interpretations that suggest that the PFZ fragments and bends the depocenters of those basins, as it has been proposed for the antiforms (ranges) that are located eastwards. Furthermore, the gravity anomaly models show that the PFZ extends from the Cabrera Range to the Almagrera Range and ends in the north at the Pulpí Basin, where the basin infill is only deformed by a gentle symmetrical synform. As a consequence, the PFZ is (i) confined to the southern zone, where the deformation is most intense due to the displacement of the tectonic indenter, and (ii) disconnected from the front of the Águilas Arc and the Alhama de Murcia Fault (part of the Eastern Betic Shear Zone, EBSZ). The new extend of the PFZ we have documented supposes the structural segmentation of the EBSZ and reduces both seismotectonic and structural significances of the PFZ. The study of the PFZ shows that the boundaries of the indenter are the locus for diffused deformation accommodated by local-scale faulting along with structural rotations and deflections, rather than localized strike-slip faulting along the whole indenter margin.

Keywords: tectonic indentation, strike-slip faults, Palomares Fault Zone, gravity models, Eastern Betic Shear Zone

1. Introduction

The accommodation of displacements during indenter tectonics results in large transcurrent fault zones separating continental blocks along indenter boundaries, which may extend into the hinterland, or affect the foreland (Davy and Cobbold, 1988; Mann, 2007; Sylvester, 1988; Tapponnier et al., 1982; Zweigel, 1998). These strike-slip systems have been studied worldwide, with remarkable results in the India-Asia collision (e.g., Cobbold and Davy, 1988; Tapponnier et al., 1982), in Taiwan (e.g., Lu and Malavieille, 1994; Zweigel, 1998), and in the Alps (e.g., Lickorish et al., 2002; Rosenberg et al., 2004). Additionally, it is known that fault zones located at the lateral margins of the indenter strongly affect the relief and delineate the indented block by deforming and dissecting pre-existing structures (e.g., Coppier et al., 1989; Davy and Cobbold, 1988; Estrada et al., 2018; Tapponnier et al., 1982). These fault zones are typically strike-slip in nature and are associated with structures, such as restraining and releasing bends (Mann, 2007). An example of this is the Chaman Fault Zone in Pakistan (e.g., Crupa et al., 2017, Davy and Cobbold, 1988). However, the deformation along the boundaries of the indenter can also be accommodated by transfer faults caused by fragmentation of the mountain front due to the irregular shape of the indenter, or by the progression of the indentation. In the case of rotated indenters, or corner indentations, the lateral boundary faults of the indenter may be transpressive (Lickorish et al., 2002; Zweigel, 1998). In addition, some of these faults may become inactive as a result of changes in the shape of the indentation, which may lead to accretion of material, as is the case of the Vuache Fault in the Jura Mountains (Homberg et al., 1999). These fault zones can therefore be tectonically complex and have a wide variety of geometries that still remain unresolved. That is the case of the Palomares Fault Zone (hereinafter, PFZ), located at the western boundary of the Águilas Arc in the eastern Betic Cordillera (SE Iberia, Fig. 1) (Borque et al., 2019; Gómez de la Peña et al., 2016; Gueguen et al., 1998; Palano et al., 2015; Rehault et al., 1985; Silva et al., 1993). In the Águilas Arc, the indenter block is part of the oceanic crust of the Neogene Algerian Basin that is rigid, and pushes into the deformed Internal Zones of the Betic Cordillera (Fig. 1d).

The aim of this study is to understand the evolution of the PFZ as the western shearing boundary of the Águilas Arc tectonic indentation. To this aim, the main features of the sedimentary infill geometry of the basins along this boundary are analyzed, using gravity prospecting. The gravity anomaly models provide new information on the geometry of the basins, the length of the PFZ, and its structural role in the Águilas Arc indentation process. Thus, this study of the PFZ, as part of a tectonic indentation, improves the knowledge of these tectonic settings.

2. Geological setting

The Águilas Arc and the PFZ are located in the Betic Cordillera, the northern branch of the Gibraltar Arc (Fig. 1), formed by the oblique convergence of the Eurasian and African plates (e.g., DeMets et al., 2010, Sanz de Galdeano, 1990). In the Miocene, the Alboran Domain (forming the Internal Zones of the orogen, including the basement of the Alboran Sea) collided with the Iberian and African paleomargins (External Zones) and thrust over them, forming the Gibraltar Arc (García-Dueñas and Balanyá, 1986; Platt et al., 2003). The Alboran Domain consists of continental crust that was part of a domain that was fragmented due to the opening of the oceanic Algerian Basin, during the Early Miocene (Gueguen et al., 1998; Mauffret et al., 2007; Spakman et al., 2018). The Internal Zones of the Betic Cordillera are formed by three main superimposed metamorphic complexes formed by Palaeozoic and Mesozoic rocks. These complexes are, from bottom to top: Nevado-Filabride, Alpujarride and Malaguide (Durand-Delga and Fontboté, 1980; Jabaloy-Sánchez et al., 2019; Platt and Vissers, 1989; Sanz de Galdeano, 1990).

Since the Late Tortonian, the NNW-SSE compression has become dominant over the extension, which led to the inversion of the Alboran Basin (Comas et al., 1992; Corsini et al., 2014; Galindo-Zaldivar et al., 2003; Sanz de Galdeano, 1990). This was coeval with the formation of intra-mountain basins in the Betic Cordillera, driven by the orthogonal extension to the NNW-SSE compression. Some of basins formed in the Betic Cordillera are the result of normal faulting, while in others, the basins occupy synform folds of the Betic basement that are sometimes affected by faults (later or coeval). In the later cases, the basins are bound by major E-W and NE-SW antiforms that represent the largest mountain ranges of the Cordillera. The Sorbas Basin is an example of this configuration (Fig. 1, Braga et al., 2003; Galindo-Zaldívar et al., 2003;

2019; Sanz de Galdeano, 1990). Other basins in the SE Iberia are the result of major fold and fault interactions, such as the Huércal Overa Basin (Fig. 1, Montenat and Ott d'Estevou, 1999; Pedrera et al., 2010; Silva et al., 1993; Wenzens and Wenzens, 1997).The sedimentary filling of these basins, for instance that of the Huércal Overa and Vera Basins, comprises Late Miocene detrital deposits with some levels of Messinian gypsum and coarse Plio-Quaternay fluvial-alluvial sediments (Barragán, 1997; Booth-Rea et al., 2003; Montenat and Ott d'Estevou, 1999; Völk, 1966).

Faults systems include E-W reverse faults, NW-SE normal and dextral faults, and NE-SW sinistral and normal faults, superimposed over previous structures like E-W dextral faults that developed during an early phase of WNW-ESE compression (Sanz de Galdeano, 1990). A clockwise rotation of the stress occurred during the Messinian from NW-SE to N-S compression, which rotated again anticlockwise during the Pliocene up to the present NNW-SSE orientation (Huibregtse et al., 1998; Jonk and Biermann, 2002).

The Eastern Betic Shear Zone (EBSZ) is a system of NE-SW to N-S sinistral faults, which includes the Carboneras, Palomares and Alhama de Murcia Fault Zones (Fig. 1, Borque et al., 2019; Bousquet, 1979; Silva et al., 1993). In addition to these fault systems, some areas such as the central Alboran Sea (Estrada et al., 2018; Galindo-Zaldivar et al., 2022; Tendero-Salmerón et al., 2022) and the Águilas Arc (Ercilla et al., 2022; Silva et al., 1993) were affected by tectonic indentation. This geodynamic setting led to the bending of the former structures (Coppier et al., 1989) and the deformation of sedimentary basins like the Vera Basin (Fig. 1b, Barragán, 1997; Montenat and Ott d'Estevou, 1999; Weijermars, 1987). The transition between the continental crust of the Internal Zones and the indenter that is part of the crust of the Neogene Algerian Basin (Rehault et al., 1985; Silva et al., 1993) is characterized by significant crustal thinning (Diaz et al., 2016; Mediouri et al., 2014). The northward displacement of the indenter was mainly accommodated by the sinistral PFZ and the dextral Moreras Fault (Fig. 1, Ercilla et al., 2022; Silva et al., 1993). The onset of the indentation probably took place before the Middle Miocene, or Tortonian, based on the beginning of the PFZ activity (Coppier et al., 1989; Weijermars, 1987).

The mountain ranges around the PFZ, such as the Cabrera Range in its western block and the Almagrera Range in its eastern block, are NNE-SSW oriented. For this reason, the PFZ has also been considered a transfer fault between these ranges with the thrusts located at their fronts (Fig. 1, Booth-Rea et al., 2004; Giaconia et al., 2015). The PFZ comprises several kilometric fault segments among which the Palomares Fault and the Arteal Fault are the most significant (Fig. 1c). García-Mayordomo (2005), and references therein, considered that its area of influence extends lengthwise from the eastern boundary of the Cabrera Range up to the frontal thrusts of the Águilas Arc. Offshore, the deformation also extends to the Palomares margin, where E-W and NE-SW ridges as well as sedimentary instabilities such as large-scale gravity-driven slides (e.g., Ercilla et al., 2022) are observed.

Active tectonics

The tectonic indentation is still active, as evidenced by seismicity (Fig. 2), GPS data and the uplift of the Vera and Pulpí Basins (Echeverria et al., 2013; García-Mayordomo et al., 2017; Palano et al., 2015; Stich et al., 2010; Stokes, 2008). GPS data show active NW-SE shortening that affects the entire EBSZ (Borque et al., 2019), with a radial pattern of displacements around the Águilas Arc as well as greater shortening at the western boundary of the Guadalentín Corridor (Alhama de Murcia Fault), rather than just at the Águilas Arc front (Echeverria et al., 2013; Palano et al., 2015). The Vera and Pulpí Basins and the Águilas Arc were uplifted during the Plio-Quaternary and their drainage is affected by the activity of the PFZ and the southwards tilting of the region (Booth-Rea et al., 2004; Giménez et al., 2000; Stokes and Mather, 2003). However, the uplift of the Vera Basin is lesser than that of the surrounding basins, such as the Sorbas or Pulpí Basins (Braga et al., 2003; Stokes, 2008; Stokes and Mather, 2003).

Regarding recent tectonic activity in the area, fault slip rates range from values of 1 mm/yr (e.g., Alhama de Murcia and Carrascoy Faults) to values of less than 0.1 mm/yr (e.g., the PFZ, including the Arteal Fault and the eastern flank of Almenara Range) (Ferrater et al., 2017; García Mayordomo et al., 2017; Martín-Banda et al., 2016; Silva et al., 2003). Nevertheless, some simulations take into account seismic ruptures of entire sections of the EBSZ (or propagation of the rupture through multiple faults), which would generate earthquakes with magnitudes greater than $M_W > 6.7$ (Herrero-Barbero et al., 2021). South of the PFZ, the Carboneras Fault shows dispersed seismic activity (Fig. 2) with some major historical earthquakes. It has been active since the Serravalian, with sinistral strike-slip kinematics during the Miocene and transpression during the Plio-Quaternary (Echverria et al., 2015; Giaconia et al., 2015; Rutter et al., 2012). Compared to other areas like the Alhama de Murcia Fault or the Huércal Overa Basin, where the southern termination of this fault is located, earthquakes in the Pulpí Basin are also rare (Fig. 2, Alfaro et al., 2012; Echeverria et al., 2013; Sánchez-Roldán et al., 2021; Stich et al., 2010). The M_W 5.2 Lorca earthquake of 2011 (Fig. 2, Martínez-Díaz et al., 2012) shows that the Alhama de Murcia Fault is presently transpressive. On the opposite edge of the Guadalentín Corridor, paleoseismic studies have detected paleoearthquakes with magnitudes above $M_W > 5$ in the frontal fault zone of the Almenara Range, which is considered part of the PFZ (Roquero et al., 2019). In addition, an earthquake of M_W 4.5 was recorded by the IGN into the Águilas Arc (2 February 1996, Fig. 2, data from IGN).

3. Data and methods

Field campaigns were carried out in the zone to collect geological and structural information and obtain accurate gravity field measurements, both along profiles orthogonal to the PFZ and to cover the adjacent Vera and Pulpí Basins. The geological observations aimed to: (i) check the lithologies and structures shown on the available geological maps of the area (e.g., Booth-Rea et al., 2003; 2004; Coppier et al., 1989; García-Mayordomo, 2005; Silva et al., 1993), (ii) identify the contacts between main geological units along the profiles, and (iii) find and follow fault planes of the PFZ in the vicinity of the profiles. 392 measurements of gravity were acquired, of which 231 points were used to create the three main profiles (Fig. 3), and others were used to populate the grid. In other words, 181 points (including some points of the profile tips that were located on basement outcrops) were used to interpolate a grid that provides a overview of the basins. The points were also used to compute the regional anomaly, since it is necessary to characterize the regional trend. For the profiles, the distance between points is about 200 m, on average. Profile 1 (south) includes 77 stations, profile 2 (center) includes 44 stations and profile 3 (north) includes 110 stations (Fig. 4).

Gravity measurements were acquired using a Scintrex Autograv CG-5 gravimeter with an accuracy of 1 µGal (0.001 mGal). The measurements were referenced to the Granada absolute gravity station (National Geographic Institute, IGN) by calibrating a field base near the town of Garrucha (Fig. 1). For each point the Free-Air, Bouguer and Terrain corrections were applied to calculate the Complete Bouguer anomaly by using the Oasis Montaj software and considering a standard background density of 2.67 g/cm^3. For the calculation of the terrain correction based on the methods of Kane (1962) and Nagy (1966), a digital terrain model (DTM), formed by a regular grid of 5 m width, combined with the bathymetry of the Gulf of Vera, which was sourced from the GEBCO database (https://www.gebco.net/data_and_products/gridded_bathymetry_data/) up to a distance of 100 km from the gravity measurement stations. The DTM was provided by the IGN (https://centrodedescargas.cnig.es/CentroDescargas/index.jsp).

The residual gravity anomaly map (Fig. 3c) was created by subtracting the regional anomaly map (Fig. 3b) from the complete Bouguer anomaly map (Fig. 3a) to remove deep basement variations effects and preserve the sedimentary basin influence. The regional anomaly map (Fig. 3b) was calculated using a first-order polynomial fit —as the Bouguer anomaly presents a linear trend— via the Oasis Montaj software, resulting in a residual anomaly where the 0 mGal isoline almost coincides with the boundaries of the basins. Subsequently, profiles 1, 2 and 3 were modelled taking into account the residual gravity anomaly using the GRAVMAG v1.7 software from the British Geological Survey (Pedley et al., 1993). This software generates vectorial objects whose vertexes are defined and modified by the user in a forward modelling process. The density values were estimated after testing a range of values based on the predominant lithologies of the region (Fig. 1) and standard averages values (Telford et al., 1990). Considering that part of profile 1 is close to the study area of Booth-Rea et al. (2004) that used drilling data, the sedimentary thickness of that area was used to calibrate the possible density values into the margins of standard averages values (Telford et al., 1990). The density values that were finally chosen after this process are shown in the profiles.

In order to contrast the gravity anomaly models results (Figs. 4 and 5), additional field work was carried out along the estimated trace of the PFZ. This field work was mainly located along the eastern boundary of the Pulpí Basin up to the trace of profile 3 to study the sediments-basement contact. Several structural measures of strike and dip of the foliation of the metamorphic rocks of the basement (schists, quartz-schists) were taken along this boundary.

4. Results

4.1 Gravity anomalies and models

The Complete Bouguer anomaly map (Fig. 3a) shows a SE-ward decreasing trend with some irregularities, most of which coincide with the Vera and Pulpí Basins. This regional trend is shown in the regional anomaly map (Fig. 3b). The map of the residual anomaly, which was created to highlight the geometry of the basin infills (Fig. 3c), shows three main depocenters located in the Vera, Pulpí and eastern Huércal Overa Basins. The lowest values are -7.5 mGal in the Vera Basin, -9.6 mGal in the Pulpí Basin and -11.4 mGal in the eastern Huércal Overa Basin (Fig. 3c).

The gravity models assume a density value of 2.67 g/cm^3 for the undifferentiated basement background, which is a standard value for the continental crust (Telford et al., 1990). A number of basement polygons with higher densities (2.8-2.9 g/cm^3) were placed to compensate for positive anomalies in basement areas and also due to edge effects on the boundaries of the profile. This value is consistent with metamorphic rocks with igneous intrusions, since some of these areas present igneous intrusions and mines of metallic ores (Fig. 1, field observations, Santos-García et al., 2022). The density value used for the sediments in the residual anomaly models is 2.4 g/cm^3, an average value for the basin sediments. In addition, in profile 1, a sediment polygon with a different density of 2.55 g/cm^3 has been added (Figs. 3 and 4). This polygon was created at the intersection of profile 1 with the Almanzora River, near its mouth, to take into consideration the thick deposit of Quaternary conglomerates of the Almanzora River located there.

Profile 1 (Fig. 4a) runs from the eastern end of the Filabres Range (W) to the southern end of the Almagrera Range (E), crossing the northern part of the Vera Basin and the PFZ (Figs. 1c and 3). The residual anomaly shows the lowest values in the central part of the basin, with two relevant minima of -7.5 mGal at ~9 km and ~12.5 km from the beginning of the profile, and with a maximum estimated sediment thickness of ~700 m (Fig. 4a). There are also some steps along the shape of the anomaly (at ~4 km, ~6 km and ~16.5 km) and an abrupt increase of the anomaly of 4 mGal that matches with the Arteal Fault (PFZ). In fact, the biggest step (> 200 m) occurs in that same fault (Fig. 4a). There is also a polygon of 2.55 g/cm^3 with a thickness of 50-80 m that coincides with the Almanzora River, probably related to conglomerates recently deposited in the river channel (according to our field observations and geological maps).

Profile 2 (Figs. 3 and 4b) crosses the Pulpí Basin from the Almagro Range (NW) to the Almagrera Range (SE). The curve of the residual anomaly is smooth and has no significant steps, with a minimum value of -8 mGal in the center of the basin (~5km). Thus, the sediment polygon of the model has an almost symmetrical shape with a depocenter that reaches a maximum thickness of 850 m (Fig. 4b).

Profile 3 (Figs. 3 and 5) is located in the Guadalentín Corridor and runs from the Estancias Range (NW) to the Águilas Arc (Almenara Range). The profile of the residual anomaly has several minima and maxima corresponding to the sub-basins and basement outcrops, respectively. The westernmost sub-basin has a sediment thickness of 450 m, corresponding to a minimum of -2 mGal. A step of 1.5 mGal matches the trace of the Alhama de Murcia Fault and is related to a step of the basement and an increase of the sediments thickness, while a total step of 3.5 mGal is observed from the boundary of the sediments (at ~2 km of distance) to the displacement of the Alhama de Murcia Fault (Fig. 5). The possible faults that form the boundaries of the Enmedio Range could be marked by steps in the gravity residual anomaly (at ~5.5 km and ~10 km). In the central sub-basin (from kms 10 to 17, Fig. 5), the profile highlights a central high (-0.5 mGal) that partially outcrops in the vicinity of the profile at km 14. This central sub-basin has two lows of -4 mGal (which corresponds to a polygon with ~450 m of thickness considering the final density value used) and -1.5 mGal (~180 m of thickness). In the eastern part (Fig. 5), a minimum value of -0.4 mGal, with 40 m of estimated sediment thickness, is linked to the small Tébar Basin within the Águilas Arc.

4.2. The continuation of the PFZ based on geological observations

The outcrops observed are grouped into those located in the connection area between the Pulpí Basin and the Guadalentín Corridor (group A, Fig. 6a) and those located southwards into the Pulpí Basin, along the margin of the Almagrera Range (group B, Fig. 6a). In the northern group A outcrops (Fig. 6a), the foliation of the Nevado-Filabride schists and mica-schists basement range from N0°E to N120°E. Those outcrops with strikes between N0°E to N40°E are usually steeply inclined (30°W-40°W), towards the basin (Fig. 6 b, c); the southern outcrops present more variable strikes which can be found up to N120°E, but with shallow dips, of 10°W to 15°W, with some outcrops dipping up to 30°W. In all these outcrops (group A, 9 outcrops) there is no evidence of the previously proposed (e.g., Booth-Rea et al., 2003; 2004; Coppier et al., 1989; García-Mayordomo, 2005; Silva et al., 1993) fault of kilometric length at the boundary of the basin that should have developed brittle deformations or fault rocks. In contrast, the dip of the foliation towards the basin is consistent with an angular unconformity at the basement-sediments interface (Fig. 6c).

Southwards, in the group B of outcrops (Fig. 6a), the observations were quite similar: the foliation presents low dips towards the basin (10°WNW-15°WNW), with an increase towards the south (up to 45°W). In this area the lithology changes from schists to quartz-schists and marbles, whose layers dip towards the basin approximately 40°W on average. There were less outcrops in this area and the mountain front has major irregularities (as pointed out by sinuosity data of García-Mayordomo, 2005), appearing on some isolated outcrops of metamorphic rocks of the Internal Zones surrounded by sediments. Again, no evidence of a strike-slip fault of kilometric length was found. On the contrary, there were some outcrops where the sediments were located over the Internal Zones, with an angular discordance at the base and without fracturing, nor fault planes. These sediments were just tilted towards the basin (approximately 40°NW).

The first evidence of faulting at the eastern boundary of the basin is found in the connection far to the south between the Pulpí and the Vera Basins (see location in Fig. 6a, the red square). At that point, a fault plane with strike-slip striae, 16/010, was located at the contact between the sediments and the basement. This is the northernmost evidence of strike-slip faulting along the eastern boundary of the Pulpí Basin that was found during the study.

5. Discussion

5.1 Alternative interpretation of the PFZ geometry

The PFZ was expected to be the main conditioning factor for the depocenters of the Pulpí and Vera Basins, because they are considered to be wrench fault basins (e.g., Jonk and Biermann, 2002; Montenat and Ott d'Estevou, 1999; Weijermars, 1987). However, gravity anomalies (Fig. 3c) show that the major depocenters of the Vera and Pulpí Basins are centered in the basins far away from the PFZ and the mountain front. This geometry suggests that they are not mainly conditioned by the PFZ, as could be expected for wrench fault basins. Only in the Vera Basin, the PFZ has generated significant subsidence, with a step of up to 200 m on the eastern boundary (Fig. 4a), which can be related to the movement of the Arteal Fault (Booth-Rea et al., 2003) and the displacement of the Almagrera Range antiform (Coppier et al., 1989; Silva et al., 1993). Nevertheless, the Vera depocenter is located up to 4 km west of the PFZ (Figs. 3c and 4a) and sediments are up to 350 m thicker than in the fault zone.

To the north, the influence of the PFZ on the development of the basin decreases, as evidenced by profile 2 (Fig. 4b), which shows a basement geometry similar to a smooth synform filled by sediments without any steps associated with the mountain front, where faulting is expected to occur (Fig. 4b). Moreover, our field observations (Fig. 6) show that there is no evidence of faulting along the eastern margin of Pulpí Basin. In contrast, previous studies (e.g., Booth-Rea et al., 2003; Silva et al., 2003) found that the fault zone could be 3.5 km wide there, from the northern tip of the segment called Palomares Fault to the segment called Arteal Fault, the western boundary of Almagrera Range. Thus, it is likely that the PFZ does not reach this part of the Pulpí Basin or, alternatively, it does not have significant influence in the basin geometry.

Further northwards, in the connection between the Pulpí Basin and the Guadalentín Corridor, the tectonic influence of the PFZ that should affect the geometry of the basin, as it is observed in the Vera Basin, is absent. This is evidenced by profile 3, where the main gravity anomaly step is related to the Alhama de Murcia, close to the boundary of the sedimentary basin, with uplifted Late Miocene sediments (Santos-García et al., 2022) in the north-western block (Fig. 5, km ~4). The thinning of these elevated sediments has an associated step of 2 mGal, which could be related to an ancient surface of the Alhama de Murcia Fault. However, along the profile, the alternation of small basins and basement outcrops is more easily interpreted as a succession of antiforms and synforms filled by sediments, with the exception of the boundaries of the Enmedio Range, which can be interpreted as faults. This could be the origin of the basement high located at the km ~14 in profile 3 (Fig. 5). Alternatively, it could also be interpreted as a blind thrust, due to its asymmetry. Consequently, the basement highs may be the result of a combination of faults and folds. The front of the Águilas Arc could be related to a step of 1 mGal at km ~16 on profile 3. This may represent a fold or, alternatively, a fault that has little or no influence on the sedimentary infill and may be covered by a thin layer of sediments, in a setting similar to the faults described by Roquero et al. (2019) in that zone.

5.2 Activity of the PFZ

Although pure strike-slip faults may not exhibit significant vertical displacements, their development in the boundary of an indenter in a collisional setting should involve areas of transpression and transtension that produce vertical displacements. Field research suggests that the PFZ acted as a normal fault in the Pliocene (García-Mayordomo, 2005; Huibregtse et al., 1998; Jonk and Biermann, 2002). Moreover, the lower uplift of the Vera Basin with respect to the surrounding basins is attributed to the activity of the PFZ segment called Palomares Fault (Booth-Rea et al., 2003; Braga et al., 2003; García-Mayordomo, 2005; Stokes, 2008; Stokes and Mather, 2003) supporting the finding that this segment has been activated during Pliocene to Quaternary. In contrast, the lack of significant changes in the thickness of the sedimentary infill in the Pulpí Basin (Profile 2, Fig. 4b) and the field observations made along the eastern boundary (Fig. 6) indicate that the PFZ is disconnected from the northern sector of the Águilas Arc mountain front (western boundary of Almenara Range). This is contrary to what has been interpreted up to this time (e.g., Bousquet et al., 1979; García-Mayordomo, 2005; García-Mayordomo et al., 2017; Weijermars, 1987). In summary, the gravity models show that the PFZ is shorter than what would be expected based on the continuity of the mountain fronts of the Almagrera Range and Almenara Range, which is mainly related to a succession of folds. This is also corroborated by field observations along the eastern boundary of the Pulpí Basin, which show foliation of the Internal Zones with a dip towards the basin (Fig. 6). Moreover, it is consistent with the low number of earthquakes in the Pulpí Basin in the last 30 years compared to the surrounding areas (Fig. 2). The uplift of the Pulpí Basin (Wenzens and Wenzens, 1997) could also have been mostly driven by other processes, such as the uplift of the surroundings ranges, rather than by recent PFZ activity (less than 0.1 mm/yr, Herrero-Barbero et al., 2021).

In this area, estimates and simulations of earthquakes of magnitude $M_W > 6.7$ due to ruptures longer than 15-20 km have been considered (e.g., García-Mayordomo et al., 2017; Herrero-Barbero et al., 2021). These assessments assume fault propagation along the EBSZ and/or include the entire PFZ with a single rupture encompassing the presumed total length of the fault from the northern Almenara Range to Cabrera Range (more than 35 km). However, based on the gravity modelling results and field observations of the PFZ, part of the EBSZ cannot be assumed to be continuous, at least in the area of the Pulpí Basin. It seems that there are no strike-slip faults that can connect the Alhama de Murcia Fault (or the Enmedio Range faults) with the PFZ, nor there are any continuation between the PFZ and the Almenara Range front (Fig. 1b). Thus, the magnitude estimations of a potential earthquake caused by the whole PFZ, or rupture propagation from the PFZ towards the north, might be overestimated.

5.3 Implications of the PFZ on the Águilas Arc indenter deformation

The PFZ can be interpreted as a strike-slip fault that has accommodated the indentation of the Águilas Arc (e.g., Ercilla et al., 2022; Silva et al., 1993) and is the result of a shear zone that has fragmented and rotated the folds of the Betic Internal Zones (e.g., Coppier et al., 1989; Jonk and Biermann, 2002). The fault can also be classified as a transfer fault between Cabrera Range and Almagrera Range (e.g., Booth-Rea et al., 2004; Giaconia et al., 2015). The shorter PFZ length estimated, according to our results, implies that the role of block rotations and/or ductile deformation must have been more significant than previously thought in the accommodation of the northwards displacement of the indenter in the Águilas Arc. The bending of previous structures and rotations, such as folds (Coppier et al., 1989; Jonk and Biermann, 2002; Silva et al., 1993; Weijermars, 1987), could have been previous to the PFZ formation. The PFZ length could have been more constrained by the fragmentation of the rotated folds, while the indentation progressed and the deformation in the indenter boundary was accumulated. This would explain its length from the Cabrera Range to the southern edge of the Pulpí Basin. According to gravity results, the Vera and Pulpí Basins could correspond to rotated parts of basement that presents a geometry similar to synforms (Fig. 7), as the Cabrera Range and Almagrera range are considered rotated and deformed antiforms (e.g., Coppier et al., 1989; Jonk and Biermann, 2002). In the case of the Vera Basin, that piece of basement with a synform geometry would have been affected by the PFZ and other basement faults (Figs. 4a and 7). Notwithstanding, fold rotations would have been the main mechanism controlling the configuration of the Pulpí and Vera Basins rather than faulting along the PFZ, which is a consequence of shear deformation along the indenter boundary.

At present times, the GPS data (Echeverria et al., 2013; Palano et al., 2015) suggest a corner indentation model that is closer to the one described by Zweigel (1998), with transpression on the boundaries, rather than the model of Tapponier et al. (1982) applied to the Águilas Arc by Silva et al. (1993), which only considers strike-slip displacement in the boundaries of the indenter. This better explains the transpression and GPS radial displacement pattern across the Águilas Arc (Borque et al., 2019; Echeverria et al., 2013; Palano et al., 2015) and the transpression on the Carboneras Fault (Echeverria et al., 2015; Rutter et al., 2012). The low seismicity in the Vera and Pulpí Basins compared to the Huércal Overa Basin and the Alhama de Murcia Fault (Fig. 2, Alfaro et al., 2012; Echeverria et al., 2013; Herrero-Barbero et al., 2021; Sánchez-Roldán et al., 2021; Silva et al., 2003) could indicate a northwesterly displacement of the deformation front of the indentation, making it so that these basins would not currently be experiencing deformation. Alternatively, the compression in the Vera and Pulpí Basins could be accommodated by folding, although field observations in these regions of low incised relief do not provide evidence of major folds in the sedimentary infill and need more detailed subsurface data to be adequately analyzed. The transpressional earthquakes such as the 2011 Lorca earthquake (Martínez-Díaz et al., 2012; Sánchez-Roldán et al., 2021) would be related to compression of the northwest-trending indentation (Fig. 7), in combination with the Eastern-Betic Shear Zone lateral movement. In addition, Roquero et al. (2019) found faults in the Guadalentín Corridor that were active during the Pleistocene, but sealed by a mature calcrete. Thus, this area may have experienced compression with folding, at least until recent times (Fig. 7), as shown by Profile 3 (Fig. 5). This could indicate a progressive inactivation of the frontal faults of the Almenara Range and a northwestward propagation of the deformation towards the Enmedio Range and the southern part of the Alhama de Murcia Fault.

The evolution of the Águilas Arc indentation into a corner indentation, and the migration of the deformation towards the northwest, could lead to the blocking of the PFZ in the future. This is supported by recent estimates of low slip rates (Herrero-Barbero et al., 2021, and references therein), GPS data (e.g., Echeverria et al., 2013; Borque et al., 2019) and earthquake distribution (Fig.2, García-Mayordomo, 2005; Herrero-Barbero et al., 2021; Silva et al., 2003). The PFZ could develop in a similar way to the Vauche Fault in the Jura Mountains (Homberg et al., 1999), and the Pulpí, Vera and part of the Guadalentín Corridor basins could be included in the indenter, if indentation progresses in the future. This process has already occurred on the Terreros Fault and in the sub-basins of the Águilas Arc (such as the Tébar Basin, profile 3, Fig. 5), as suggested by Coppier et al. (1989). The lower uplift of the Vera Basin (Braga et al., 2003; Stokes, 2008) may also be related to its location south of the indentation front, which implies less compression than on the Águilas Arc front.

6. Conclusions

This study offers new insights and alternative interpretations in the formation of strike-slip fault zones and basins that develop in the framework of tectonic indentation based on gravimetric surveys and structural data. The western boundary of the Águilas Arc indenter (SE Iberian Peninsula) and the sedimentary basins located to the west is determined by a NNE-SSW mountain front that, up until today, have been thought to be formed by the Palomares Fault zone. New gravity data demonstrate that the depocenters of the Vera and Pulpí Basins are located in their central parts, associated with basement geometries that seem to be synforms. In the south, only the eastern boundary of the Vera Basin has been clearly influenced by the PFZ, showing a stepped fold and a vertical contact (the Arteal Fault, which is part of the PFZ). In the central sector, the Pulpí Basin is characterized by a basement geometry that points to a symmetrical synform with no evidence of major faults. In the northern sector, the main deformation is represented by folds (including basement highs such as the Enmedio Range) and the Alhama de Murcia Fault along the western part of the Guadalentín Corridor. Thus, the EBSZ faults seem to show a discontinuity between the

PFZ in the Vera Basin and the strike-slip faults in the Guadalentín Corridor, with a disconnection at the Pulpí Basin. In any case, the deformation is accommodated by folds along the boundary.

The length of the PFZ is constrained by the deformation, fragmentation and rotation of the folds of the Betic Internal Zones, specifically the antiforms of the Almagrera and Cabrera ranges. The adjacent Vera and Pulpí Basins are the result of the corresponding rotated and fragmented basement synform, which has been filled by the sediments of these basins. These fold rotations are caused by the tectonic indentation of a rigid fragment of the oceanic crust of the Algerian Basin into the eastern Betics. The present-day deformation field from the GPS data and seismicity indicates NW migration of the indentation front, with consequent folding of the western Guadalentín Corridor and propagation to the Alhama de Murcia Fault. In this context, the activity of the PFZ decreases and the Vera Basin experiences a low rate of uplift.

The current Eurasia-Africa convergence has led to corner indentation with transpression at the margins, as proposed in the model of Zweigel (1998) for the Carpathian region, or the model of Lickorish et al. (2002) for the western Alps. However, in contrast with the well-known models of indentation tectonics, the Águilas Arc indentation developed folds along the boundary and the fold axis are rotated (like the Cabrera and Almagrera ranges). As the shearing deformation increased, several fractures were generated that accommodate the indenter displacement, rather than the generation of large strike-slip systems. Then, instead of a continuous strike-slip fault zone, a discontinuous one has been formed with areas where the whole deformation is accommodated by rotation and, likely, by ductile processes. These characteristics, and the fact that the indenter is a block of young, rigid oceanic crust that compresses a thin and deformed continental domain, makes the PFZ and the Águilas Arc an interesting case study for tectonic indentation processes.

Acknowledgments

This study was supported by projects CGL2016-80687-R AEI/FEDER, PID2022-136678NB-I00, AEI /FEDER, P18-RT-3275, B-RNM-301-UGR18 and RNM148 (Junta de Andalucía/FEDER). V.T.S. was supported by the FPU PhD grant (16/04038). ICM-CSIC author acknowledges the Severo Ochoa funding from the Spanish government through the "Severo Ochoa Centre of Excellence" accreditation (CEX2019-000928-S). The authors also acknowledge the comments, suggestions and contributions of both reviewers, which have significantly improved the study.

References

Alfaro, P., Bartolomé, R., Borque Arancón, M. J., Estévez, A., García Mayordomo, J., García-Tortosa, F. J., ... & Lo Iacono, C. (2012). The Bajo Segura fault zone: active blind thrusting in the eastern betic cordillera (SE Spain). *Journal of Iberian Geology, 38*(1), 271-284. http://dx.doi.org/10.5209/rev_JIGE.2012.v38.n1.39217

Barragán, G. (1997). *Evolución geodinámica de la depresión de Vera: provincia de Vera*. (Doctoral dissertation). Universidad de Granada.

Booth-Rea, G., Azañón, J. M., García-Dueñas, V., & Augier, R. (2003). Uppermost Tortonian to Quaternary depocentre migration related with segmentation of the strike-slip Palomares Fault Zone, Vera Basin (SE Spain). *Comptes Rendus Geoscience*, *335*(9), 751-761.

Booth-Rea, G., Azañón, J. M., Azor, A., & García-Dueñas, V. (2004). Influence of strike-slip fault segmentation on drainage evolution and topography. A case study: the Palomares Fault Zone (southeastern Betics, Spain). *Journal of Structural Geology*, *26*(9), 1615-1632.

Borque, M. J., Sánchez-Alzola, A., Martin-Rojas, I., Alfaro, P., Molina, S., Rosa-Cintas, S., ... & Gil, A. J. (2019). How much Nubia-Eurasia convergence is accommodated by the NE end of the Eastern Betic Shear Zone (SE Spain)? Constraints from GPS velocities. *Tectonics*, *38*(5), 1824-1839.

Bousquet, J. C. (1979). Quaternary strike-slip faults in southeastern Spain. *Tectonophysics*, *52*(1-4), 277-286.

Braga, J. C., Martín, J. M., & Quesada, C. (2003). Patterns and average rates of late Neogene–Recent uplift of the Betic Cordillera, SE Spain. *Geomorphology*, *50*(1-3), 3-26.

Cobbold, P. R., & Davy, P. H. (1988). Indentation tectonics in nature and experiment. II: Central Asia. *Bulletin of the Geological Institution of the University of Upsala*, *14*, 143-162.

Comas, M. C., García-Dueñas, V., & Jurado, M. J. (1992). Neogene tectonic evolution of the Alboran Sea from MCS data. *Geo-Marine Letters*, *12*(2), 157-164.

Coppier, G., Griveaud, P., de Larouzière, F. D., Montenat, C., & Ott d'Estevou, P. (1989). Example of Neogene tectonic indentation in the Eastern Betic Cordilleras: the Arc of Águilas (southeastern Spain). *Geodinamica Acta*, *3*(1), 37-51.

Corsini, M., Chalouan, A., & Galindo-Zaldivar, J. (2014). Geodynamics of the Gibraltar Arc and the Alboran Sea region. *J. Geodyn., 77*, 1–3. https://doi.org/10.1016/j. jog.2014.04.005

Crupa, W. E., Khan, S. D., Huang, J., Khan, A. S., & Kasi, A. (2017). Active tectonic deformation of the western Indian plate boundary: A case study from the Chaman Fault System. *Journal of Asian Earth Sciences*, *147*, 452-468.

Davy, P., & Cobbold, P. R. (1988). Indentation tectonics in nature and experiment. 1. Experiments scaled for gravity. Bull. Geol. Inst. Univ. Uppsala, 14, 129-141.

De Larouzière, F. D., Bolze, J., Bordet, P., Hernandez, J., Montenat, C., & d'Estevou, P. O. (1988). The Betic segment of the lithospheric Trans-Alboran shear zone during the Late Miocene. *Tectonophysics*, *152*(1-2), 41-52.

DeMets, C., Gordon, R. G., & Argus, D. F. (2010). Geologically current plate motions. *Geophysical Journal International*, *181*(1), 1–80. https://doi.org/10.1111/j.1365-246X.2009.04491.x

Diaz, J., Gallart, J., & Carbonell, R. (2016). Moho topography beneath the Iberian-Western Mediterranean region mapped from controlled-source and natural seismicity surveys. *Tectonophysics*, *692*, 74-85.

Durand Delga, M., & Fontboté, J.M. (1980). Le cadre structural de la Méditerranée occidentale. *Mém. B.R.G.M. 115*, 67–85.

Echeverria, A., Khazaradze, G., Asensio, E., Gárate, J., Dávila, J. M., & Suriñach, E. (2013). Crustal deformation in eastern Betics from CuaTeNeo GPS network. *Tectonophysics*, *608*, 600-612.

Echeverria, A., Khazaradze, G., Asensio, E., & Masana, E. (2015). Geodetic evidence for continuing tectonic activity of the Carboneras fault (SE Spain). *Tectonophysics*, *663*, 302-309.

Ercilla, G., Galindo-Zaldívar, J., Estrada, F., Valencia, J., Juan, C., Casas, D., ... & Yenes, M. (2022). Understanding the complex geomorphology of a deep sea area affected by continental tectonic indentation: The case of the Gulf of Vera (Western Mediterranean). *Geomorphology*, 108126.

Estrada, F., Galindo-Zaldivar, J., Vázquez, J. T., Ercilla, G., D'Acremont, E., Alonso, B., & Gorini, C. (2018). Tectonic indentation in the central Alboran Sea (westernmost Mediterranean). *Terra Nova, 30*(1), 24-33. https://doi.org//10.1111/ter.12304

Ferrater, M., Ortuño, M., Masana, E., Martínez-Díaz, J. J., Pallàs, R., Perea, H., ... & Arrowsmith, R. (2017). Lateral slip rate of Alhama de Murcia fault (SE Iberian Peninsula) based on a morphotectonic analysis: Comparison with paleoseismological data. *Quaternary International*, *451*, 87-100.

Galindo-Zaldıvar, J., Gil, A. J., Borque, M. J., González-Lodeiro, F., Jabaloy, A., Marın-Lechado, C., ... & Sanz de Galdeano, C. (2003). Active faulting in the internal zones of the central Betic Cordilleras (SE, Spain). *Journal of Geodynamics*, *36*(1-2), 239-250. https://doi.org/10.1016/S0264-3707(03)00049-8

Galindo-Zaldívar, J., Braga, J. C., Marín-Lechado, C., Ercilla, G., Martín, J. M., Pedrera, A., ... & Alonso, B. (2019). Extension in the Western Mediterranean. In *The geology of Iberia: a geodynamic approach* (pp. 61-103). Springer, Cham.

Galindo-Zaldivar, J., Gil, A. J., Tendero-Salmerón, V., Borque, M. J., Ercilla, G., González-Castillo, L., ... & Chacón, F. (2022). The Campo de Dalias GNSS Network Unveils the Interaction between Roll-Back and Indentation Tectonics in the Gibraltar Arc. *Sensors*, *22*(6), 2128.

García-Dueñas, V., & Balanyá, J. C. (1986). Estructura y naturaleza del Arco de Gibraltar. *Maleo Bolletin. Societa Geologica del Portugal*, *2*, 23.

García-Mayordomo, J. (2005). *Caracterización y Análisis de la Peligrosidad Sísmica en el Sureste de España.* Doctoral dissertation. Universidad Complutense de Madrid.

García-Mayordomo, J., Martín-Banda, R., Insua-Arévalo, J. M., Álvarez-Gómez, J. A., Martínez-Díaz, J. J., & Cabral, J. (2017). Active fault databases: building a bridge between earthquake geologists and seismic hazard practitioners, the case of the QAFI v. 3 database. *Natural Hazards and Earth System Sciences*, *17*(8), 1447-1459.

Giaconia, F., Booth-Rea, G., Martínez-Martínez, J. M., Azañón, J. M., & Pérez-Peña, J. V. (2012). Geomorphic analysis of the Sierra Cabrera, an active pop-up in the constrictional domain of conjugate strike-slip faults: The Palomares and Polopos fault zones (eastern Betics, SE Spain). *Tectonophysics*, *580*, 27-42.

Giaconia, F., Booth-Rea, G., Ranero, C. R., Gràcia, E., Bartolome, R., Calahorrano, A., ... & Viñas, M. (2015). Compressional tectonic inversion of the Algero-Balearic basin: Latemost Miocene to present oblique convergence at the Palomares margin (Western Mediterranean). *Tectonics*, *34*(7), 1516-1543.

Giménez, J., Suriñach, E., & Goula, X. (2000). Quantification of vertical movements in the eastern Betics (Spain) by comparing levelling data. *Tectonophysics*, *317*(3-4), 237-258.

Gómez de la Peña, L., Gràcia, E., Muñoz, A., Acosta, J., Gómez-Ballesteros, M., Ranero, C. R., & Uchupi, E. (2016). Geomorphology and Neogene tectonic evolution of the Palomares continental margin (Western Mediterranean). *Tectonophysics*, *689*, 25-39.

Gueguen, E., Doglioni, C., & Fernandez, M. (1998). On the post-25 Ma geodynamic evolution of the western Mediterranean. *Tectonophysics, 298*(1-3), 259–269. https://doi.org/10.1016/S0040-1951(98)00189-9.

Herrero-Barbero, P., Álvarez-Gómez, J. A., Williams, C., Villamor, P., Insua-Arévalo, J. M., Alonso-Henar, J., & Martínez-Díaz, J. J. (2021). Physics-Based Earthquake Simulations in Slow-Moving Faults: A Case Study From the Eastern Betic Shear Zone (SE Iberian Peninsula). *Journal of Geophysical Research: Solid Earth*, *126*(5), e2020JB021133.

Homberg, C., Lacombe, O., Angelier, J., & Bergerat, F. (1999). New constraints for indentation mechanisms in arcuate belts from the Jura Mountains, France. *Geology*, *27*(9), 827-830.

Huibregtse, P., van Alebeek, H., Zaal, M., & Biermann, C. (1998). Palaeostress analysis of the northern Nijar and southern Vera basins: constraints for the Neogene displacement history of major strike-slip faults in the Betic Cordilleras, SE Spain. *Tectonophysics*, *300*(1-4), 79-101.

Jabaloy-Sánchez, A., Martín-Algarra, A., Padrón-Navarta, J. A., Martín-Martín, M., Gómez-Pugnaire, M. T., Sánchez-Vizcaíno, V. L., & Garrido, C. J. (2019). Lithological successions of the Internal Zones and Flysch Trough units of the Betic Chain. In *The Geology of Iberia: A Geodynamic Approach* (pp. 377-432). Springer, Cham. https://doi.org/10.1007/978-3-030-11295-0_8

Jonk, R., & Biermann, C. (2002). Deformation in Neogene sediments of the Sorbas and Vera Basins (SE Spain): constraints on simple-shear deformation and rigid body rotation along major strike-slip faults. *Journal of Structural Geology*, *24*(5), 963-977.

Kane, M. (1962). A comprehensive system of terrain corrections using a digital computer. *Geophysics*, *27*(4), 455–462. https://doi.org/ 10.1190/1.1439044

Lickorish, W. H., Ford, M., Burgisser, J., & Cobbold, P. R. (2002). Arcuate thrust systems in sandbox experiments: A comparison to the external arcs of the Western Alps. *Geological Society of America Bulletin*, *114*(9), 1089-1107.

Lu, C. Y., & Malavieille, J. (1994). Oblique convergence, indentation and rotation tectonics in the Taiwan Mountain Belt: Insights from experimental modelling. *Earth and Planetary Science Letters*, *121*(3-4), 477-494.

Mann, P. (2007). Global catalogue, classification and tectonic origins of restraining-and releasing bends on active and ancient strike-slip fault systems. *Geological Society, London, Special Publications*, *290*(1), 13-142.

Martín-Banda, R., García-Mayordomo, J., Insua-Arévalo, J. M., Salazar, Á. E., Rodríguez-Escudero, E., Álvarez-Gómez, J. A., ... & Herrero, M. J. (2016). New insights on the seismogenic potential of the Eastern Betic Shear Zone (SE Iberia): Quaternary activity and paleoseismicity of the SW segment of the Carrascoy Fault Zone. *Tectonics*, *35*(1), 55-75.

Martínez-Díaz, J. J., Bejar-Pizarro, M., Álvarez-Gómez, J. A., de Lis Mancilla, F., Stich, D., Herrera, G., & Morales, J. (2012). Tectonic and seismic implications of an intersegment rupture: The damaging May 11th 2011 Mw 5.2 Lorca, Spain, earthquake. *Tectonophysics*, *546*, 28-37.

Medaouri, M., Déverchère, J., Graindorge, D., Bracene, R., Badji, R., Ouabadi, A., ... & Bendiab, F. (2014). The transition from Alboran to Algerian basins (Western Mediterranean Sea): chronostratigraphy, deep crustal structure and tectonic evolution at the rear of a narrow slab rollback system. *Journal of Geodynamics*, *77*, 186-205.

Montenat, C., & Ott d'Estevou, P. (1999). The diversity of late Neogene sedimentary basins generated by wrench faulting in the Eastern Betic Cordillera, SE Spain. *Journal of Petroleum Geology*, *22*(1), 61-80.

Nagy, D. (1966). The gravitational attraction of a right rectangular prism. *Geophysics*, *31*(2), 362–371. https://doi.org/10.1190/1.1439779

Palano, M., González, P. J., & Fernández, J. (2015). The Diffuse Plate boundary of Nubia and Iberia in the Western Mediterranean: Crustal deformation evidence for viscous coupling and fragmented lithosphere. *Earth and Planetary Science Letters*, *430*, 439-447.

Pedley, R. C., Busby, J. P., & Dabek, Z. K. (1993). *GRAVMAG user manual-interactive 2.5 D gravity and magnetic modelling* (technical report WK/93/26/R.73). British Geological Survey.

Pedrera, A., Galindo-Zaldívar, J., Tello, A., & Marín-Lechado, C. (2010). Intramontane basin development related to contractional and extensional structure interaction at the termination of a major sinistral fault: The Huércal-Overa Basin (Eastern Betic Cordillera). *Journal of Geodynamics*, *49*(5), 271-286.

Platt, J. P., & Vissers, R. L. M. (1989). Extensional collapse of thickened continental lithosphere: A working hypothesis for the Alboran Sea and Gibraltar arc. *Geology*, *17*(6), 540–543.

Platt, J. P., Allerton, S., Kirker, A., Mandeville, C., Mayfield, A., Platzman, E. S., & Rimi, A. (2003). The ultimate arc: Differential displacement, oroclinal bending, and vertical axis rotation in the External Betic-Rif arc. *Tectonics*, *22*(3).

Rehault, J.P., Boillot, G., & Mauffret, A. (1985). *The Western Mediterranean Basin.* In: Stanley, D.J., Wezel, F.-C. (Eds.), *Geological Evolution of the Mediterranean Basin: Raimondo Selli Commemorative Volume.* Springer New York, New York, NY, pp. 101–129.

Roquero, E., Silva, P. G., Rodríguez-Pascua, M. A., Bardají, T., Elez, J., Carrasco-García, P., & Giner-Robles, J. L. (2019). Analysis of faulted fan surfaces and paleosols in the Palomares Fault Zone (Betic Cordillera, SE Spain): Paleoclimatic and paleoseismic implications. *Geomorphology*, *342*, 88-102.

Rosenberg, C. L., Brun, J. P., & Gapais, D. (2004). Indentation model of the Eastern Alps and the origin of the Tauern Window. *Geology*, *32*(11), 997-1000.

Rutter, E. H., Faulkner, D. R., & Burgess, R. (2012). Structure and geological history of the Carboneras Fault Zone, SE Spain: Part of a stretching transform fault system. *Journal of Structural Geology*, *45*, 68-86.

Sánchez-Roldán, J. L., Martínez-Díaz, J. J., Cantavella, J. V., Álvarez-Gómez, J. A., & Morales, J. (2021). Relocation of Seismicity in the Guadalentín Tectonic Valley, Eastern Betics Shear Zone (Southeast Iberia). *Seismological Society of America*, *92*(5), 3046-3064.

Santos-García, J. A., Booth-Rea, G., Silva, P. G., Bardají-Azcarate, T., Goy, J. L., Zazo, C., Aragón-Rueda, R., Hornero-Díaz, J. E., & Santiago-Martín, A. (2022). *Memoria del Mapa Geológico de España 1:50000 (MAGNA 3.0), Hoja de Puerto Lumbreras (975)*. Madrid, Spain: IGME.

Sanz De Galdeano, C. (1990). Geologic evolution of the Betic Cordilleras in the Western Mediterranean, Miocene to the present. *Tectonophysics*, *172*(1-2), 107–119. https://doi.org/10.1016/0040-1951(90)90062-D

Silva, P. G., Goy, J. L., Somoza, L., Zazo, C., & Bardají, T. (1993). Landscape response to strike-slip faulting linked to collisional settings: Quaternary tectonics and basin formation in the Eastern Betics, southeastern Spain. *Tectonophysics*, *224*(4), 289-303.

Silva, P. G., Goy, J. L., Zazo, C., & Bardají, T. (2003). Fault-generated mountain fronts in southeast Spain: geomorphologic assessment of tectonic and seismic activity. *Geomorphology*, *50*(1-3), 203-225.

Spakman, W., Chertova, M.V., van den Berg, A., & van Hinsbergen, D. J. (2018). Puzzling features of western Mediterranean tectonics explained by slab dragging. *Nat. Geosci.*, *11*(3), 211–216. https://doi.org/10.1038/s41561-018-0066-z.

Stokes, M. (2008). Plio-Pleistocene drainage development in an inverted sedimentary basin: Vera basin, Betic Cordillera, SE Spain. *Geomorphology*, *100*(1-2), 193-211.

Stokes, M., & Mather, A. E. (2003). Tectonic origin and evolution of a transverse drainage: the Río Almanzora, Betic Cordillera, Southeast Spain. *Geomorphology*, *50*(1-3), 59-81.

Stich, D., Martín, R., & Morales, J. (2010). Moment tensor inversion for Iberia–Maghreb earthquakes 2005–2008. *Tectonophysics*, *483*(3-4), 390-398.

Sylvester, A. G. (1988). Strike-slip faults. *Geological Society of America Bulletin*, *100*(11), 1666-1703.

Tapponnier, P., Peltzer, Le Dain, A. Y., Armijo, R., & Cobbold, P. (1982). Propagating extrusion tectonics in Asia: New insights from simple experiments with plasticine. *Geology*, *10*(12), 611-616.

Tavakoli, F., Walpersdorf, A., Authemayou, C., Nankali, H. R., Hatzfeld, D., Tatar, M., ... & Cotte, N. (2008). Distribution of the right-lateral strike–slip motion from the Main Recent Fault to the Kazerun Fault System (Zagros, Iran): Evidence from present-day GPS velocities. *Earth and Planetary Science Letters*, *275*(3-4), 342-347.

Telford, W. M., Geldart, L. P., & Sheriff, R. E. (1990). *Applied Geophysics*. Cambridge, UK. Cambridge University Press.

Tendero-Salmerón, V., Galindo-Zaldivar, J., d'Acremont, E., Catalán, M., Martos, Y. M., Ammar, A., & Ercilla, G. (2022). New insights on the Alboran Sea basin extension and continental collision from magnetic anomalies related to magmatism (western Mediterranean). *Marine Geology*, *443*, 106696.

Völk, H. R. (1966). *Geologie et stratigraphie du Bassin Neogene de Vera*. Doctoral dissertation. University of Amsterdam.

Weijermars, R. (1987). The Palomares brittle—ductile Shear Zone of southern Spain. *Journal of Structural Geology*, *9*(2), 139-157.

Wenzens, E., & Wenzens, G. (1997). The influence of tectonics, sea-level fluctuations and river capture on the Quaternary morphogenesis of the semi-arid Pulpi Basin (southeast Spain). *Catena*, *30*(4), 283-293.

Zweigel, P. (1998). Arcuate accretionary wedge formation at convex plate margin corners: results of sandbox analogue experiments. *Journal of Structural Geology*, *20*(12), 1597-1609.

Declaration of interests

☒The authors declare that they have no known competing financial interests or personal relationships that could have appeared to influence the work reported in this paper.

☐The authors declare the following financial interests/personal relationships which may be considered as potential competing interests:

Figure 1. Geological context of the study zone based on Ercilla et al. (2022). a. Tectonic plate sketch showing the location of the zone. GA: Gibraltar Arc. b. Simplified geological map of Eastern Betic Shear Zone and the Águilas Arc. The modelled profiles are also depicted. c. Zoom of the study zone. The area of Figures 2 and 3 is depicted. AF: Arteal Fault; AGR: Almagro Range; ALR: Alhamilla Range; AMF: Alhama de Murcia Fault; BSF: Bajo Segura Fault; CaF: Carrascoy Fault; CBR: Cabrera Range; CrF: Crevillente Fault; GdC: Guadalentín Corridor; HOB: Huércal Overa Basin; LTF: Los Tollos Fault; PB: Pulpí Basin; PF: Palomares Fault, SDE: Enmedio Range. d. Tectonic sketch of the indentation in the Gulf of Vera.

Figure 2. Earthquakes in SE Spain from 1990 to 2023 with magnitudes ≥ 2.5. Three focal mechanisms are shown that correspond to the Bullas earthquake (6 August 2002, M_W 5.0), Lorca earthquake (11 May 2011, M_W 5.2) and Turre earthquake (31 December 2022, M_W 4.0). Both the earthquakes locations and focal mechanisms were obtained from IGN,https://www.ign.es/web/ign/portal/sis-area-sismicidad. The main active faults are depicted. AMF: Alhama de Murcia Fault; BSF: Bajo Segura Fault; CaF: Carrascoy Fault; CrF: Crevillente Fault; GdC: Guadalentín Corridor; HOB: Huércal Overa Basin; LTF: Los Tollos Fault.

Figure 3. Maps of the Complete Bouguer anomaly (a), modelled regional gravity anomaly (b) and residual gravity anomaly (c) of the study zone with the approximated basin boundaries (dashed orange lines). The gravity stations are marked as black dots and the modeled profiles, orthogonal to the PFZ and the mountain front of the Águilas Arc, are depicted. CBR: Cabrera Range.

Figure 4. Gravity models of profile 1 (a) and 2 (b). The locations of the profiles are indicated in Figs. 1b, c and 3c. AF: Arteal Fault; PFZ: Palomares Fault Zone. The RMSE (root mean squared error) value for each profile is depicted.

Figure 5. Gravity model of profile 3 with a vertical exaggeration (VE x2). The location of the profile is indicated in Figs. 1b, c and 3c. The proposed blind thrust below the Guadalentín Corridor is depicted. AMF: Alhama de Murcia Fault. The RMSE (root mean squared error) value of the profile is depicted.

Figure 6. Field observations along the eastern margin of the Pulpí Basin. a. Geological map with the location of the photographs, the trace of the gravity anomaly profiles (in orange) and the strike and dip measures of the foliation. b. Panoramic view on the basin boundary at the connection between Pulpí and Guadalentín basins. c. Detail of the sediments-schists contact at that point.

Figure 7. The Palomares Fault Zone in the frame of the tectonic sketch of the evolution of the Águilas Arc based on Coppier et al. (1989). The data used for the yellow arrows are based on the geodetic results of Borque et al. (2019) and Echeverria et al. (2013, 2015). The traces of synforms and antiforms represent the main trend of the real folds. AGR: Almagro Range; AMF: Alhama de Murcia Fault; AR: Almagrera Range; CbF: Carboneras Fault; CBR: Cabrera Range; FR: Filabres Range; HOB: Huércal Overa Basin; PFZ: Palomares Fault Zone; PB: Pulpí Basin; TF: Terreros Fault; VB: Vera Basin.

Highlights

New gravity data characterize the geometry of the basins next to the Palomares fault

Palomares fault does not extend to the Pulpí basin that has a shape of gentle synform

Models point to a migration of the deformation NW-wards of the Águilas Arc

Shearing along the indenter boundary rotated folds instead of forming a large fault

The length of the Palomares fault is constrained by folds rotation and deformation

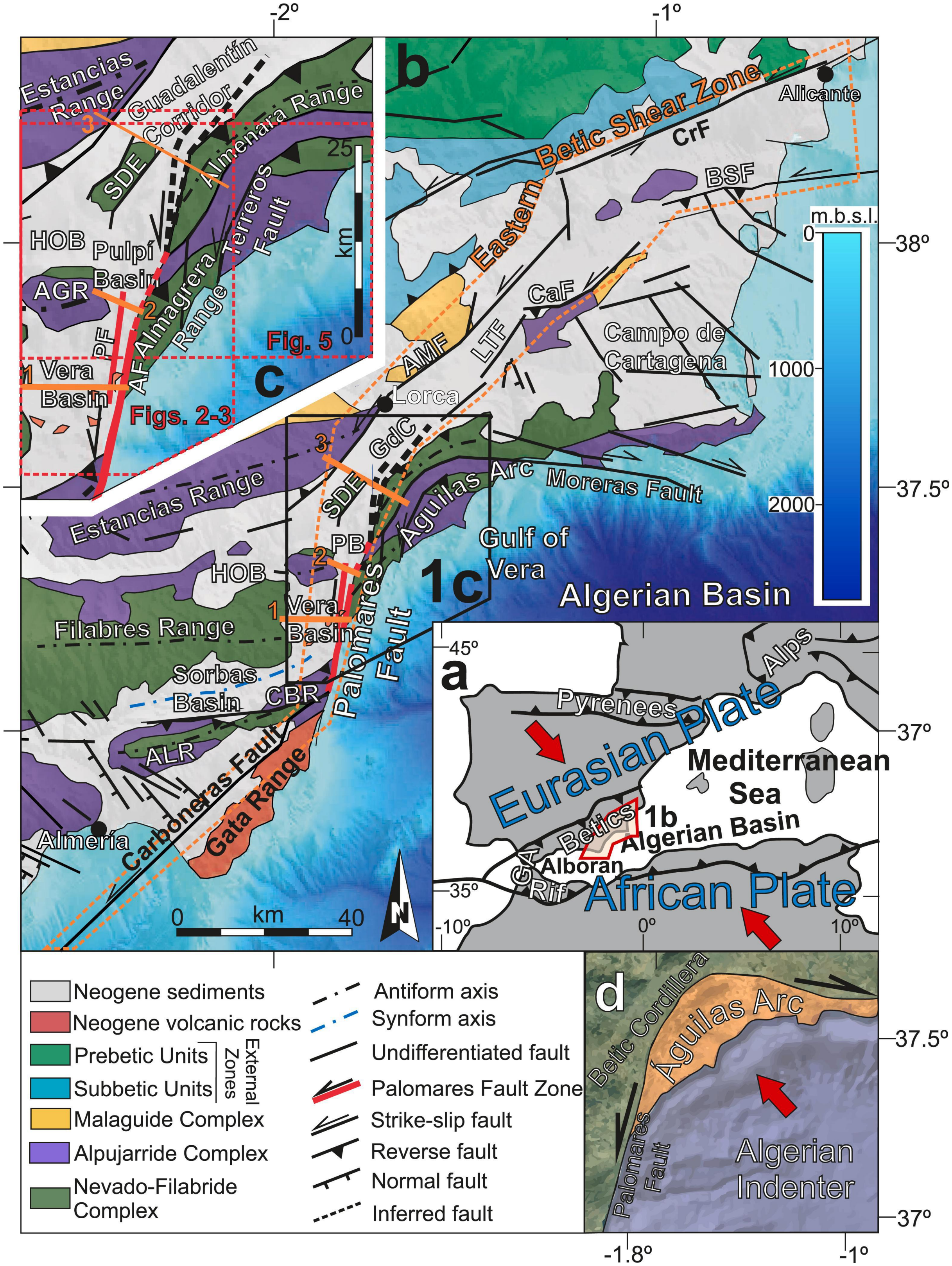
-2º
-1º
b
Estancias Range
Guadalentín Corridor
Almenara Range
SDE
HOB
Pulpí Basin
AGR
Terreros Fault
Almagrera Range
PF
AF
Vera Basin
Fig. 5
Figs. 2-3
c
25
km
0
Eastern Betic Shear Zone
Alicante
CrF
BSF
CaF
AMF
LTF
Campo de Cartagena
Lorca
GdC
Águilas Arc
Moreras Fault
PB
Gulf of Vera
1c
Algerian Basin
Palomares Fault
Filabres Range
Sorbas Basin
CBR
ALR
Carboneras Fault
Gata Range
Almería
0 km 40
N
m.b.s.l.
0
1000
2000
38º
37.5º
37º
a
45º
Alps
Pyrenees
Eurasian Plate
Mediterranean Sea
Betics
1b
Algerian Basin
Alboran
GA
Rif
African Plate
35º
-10º
0º
10º
Neogene sediments
Neogene volcanic rocks
Prebetic Units
Subbetic Units
External Zones
Malaguide Complex
Alpujarride Complex
Nevado-Filabride Complex
Antiform axis
Synform axis
Undifferentiated fault
Palomares Fault Zone
Strike-slip fault
Reverse fault
Normal fault
Inferred fault
d
Betic Cordillera
Águilas Arc
Palomares Fault
Algerian Indenter
37.5º
37º
-1.8º
-1º

Figure 1

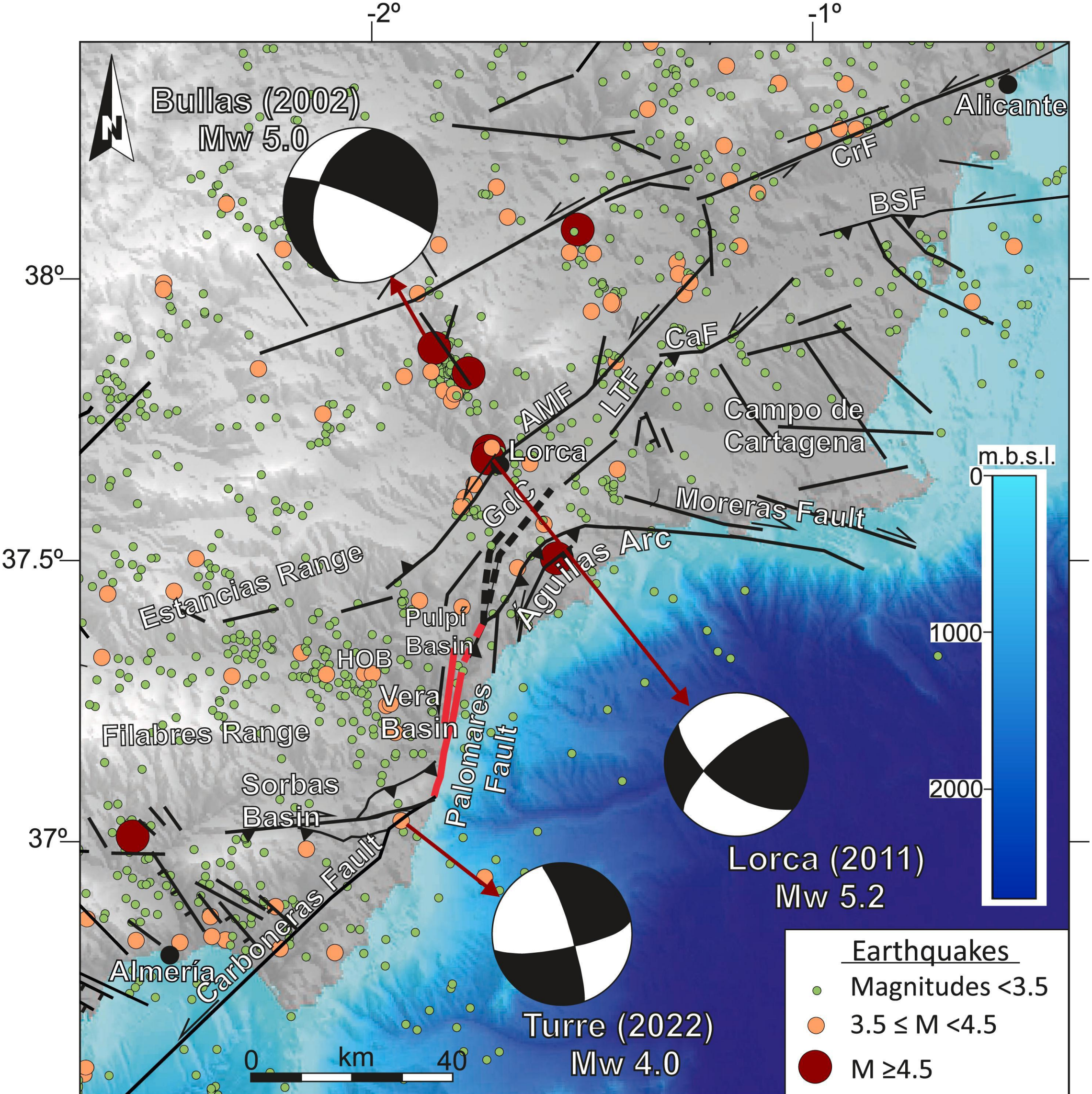

-2º
-1º
38º
37.5º
37º
N
Bullas (2002)
Mw 5.0
Alicante
CrF
BSF
CaF
AMF
LTF
Campo de
Cartagena
Lorca
m.b.s.l.
0
1000
2000
GdC
Moreras Fault
Águilas Arc
Estancias Range
Pulpí
Basin
HOB
Vera
Basin
Palomares
Fault
Filabres Range
Sorbas
Basin
Carboneras Fault
Almería
Lorca (2011)
Mw 5.2
Turre (2022)
Mw 4.0
0
km
40
Earthquakes
Magnitudes <3.5
3.5 ≤ M <4.5
M ≥4.5

Figure 2

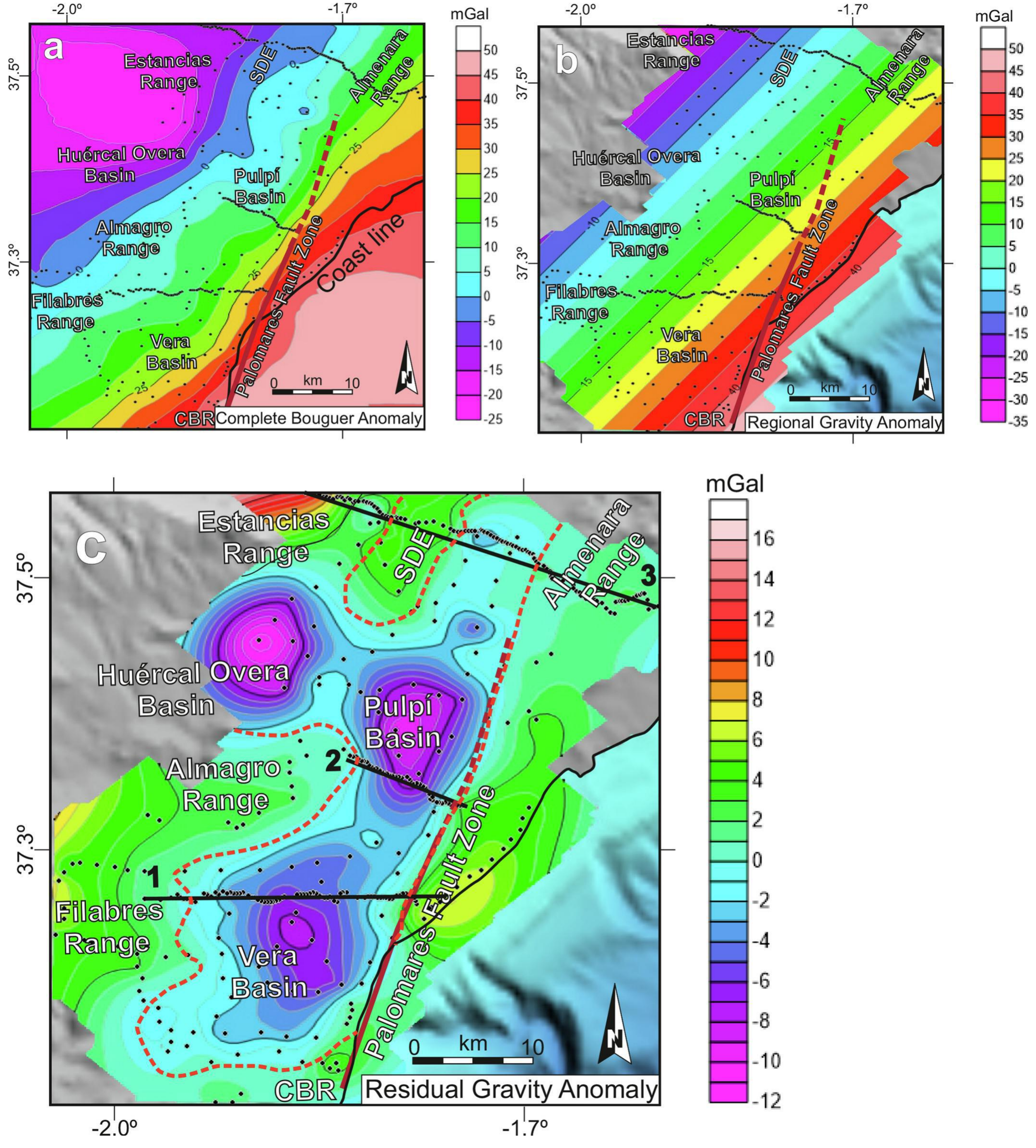
a
Estancias Range
SDE
Almenara Range
Huércal Overa Basin
Pulpí Basin
Almagro Range
Filabres Range
Vera Basin
Palomares Fault Zone
Coast line
CBR
Complete Bouguer Anomaly
mGal
b
Regional Gravity Anomaly
c
Residual Gravity Anomaly
-2.0º
-1.7º
37.5º
37.3º

Figure 3

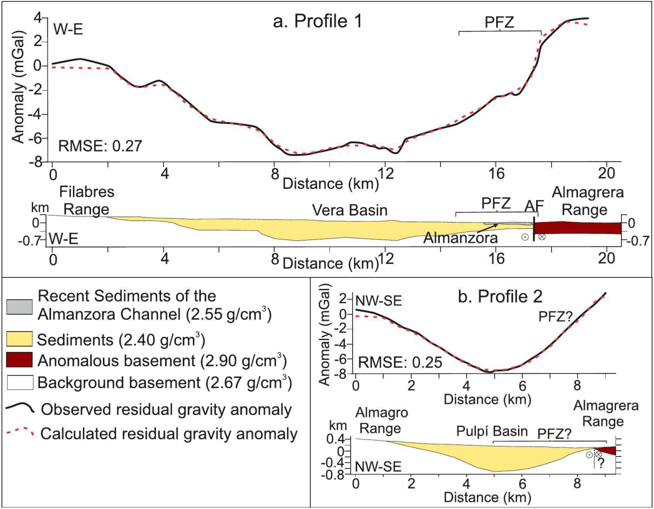
a. Profile 1
W-E
PFZ
Anomaly (mGal)
RMSE: 0.27
Distance (km)
Filabres Range
km
Vera Basin
PFZ
AF
Almagrera Range
Almanzora
W-E
Distance (km)
Recent Sediments of the Almanzora Channel (2.55 g/cm³)
Sediments (2.40 g/cm³)
Anomalous basement (2.90 g/cm³)
Background basement (2.67 g/cm³)
Observed residual gravity anomaly
Calculated residual gravity anomaly
b. Profile 2
NW-SE
PFZ?
Anomaly (mGal)
RMSE: 0.25
Distance (km)
Almagro Range
km
Pulpí Basin
PFZ?
Almagrera Range
NW-SE
Distance (km)

Figure 4

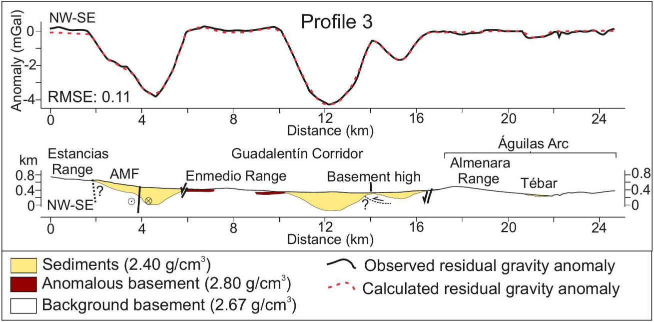
Profile 3
NW-SE
Anomaly (mGal)
RMSE: 0.11
Distance (km)
km
Estancias Range
AMF
Enmedio Range
Guadalentín Corridor
Basement high
Águilas Arc
Almenara Range
Tébar
NW-SE
Sediments (2.40 g/cm3)
Anomalous basement (2.80 g/cm3)
Background basement (2.67 g/cm3)
Observed residual gravity anomaly
Calculated residual gravity anomaly

Figure 5

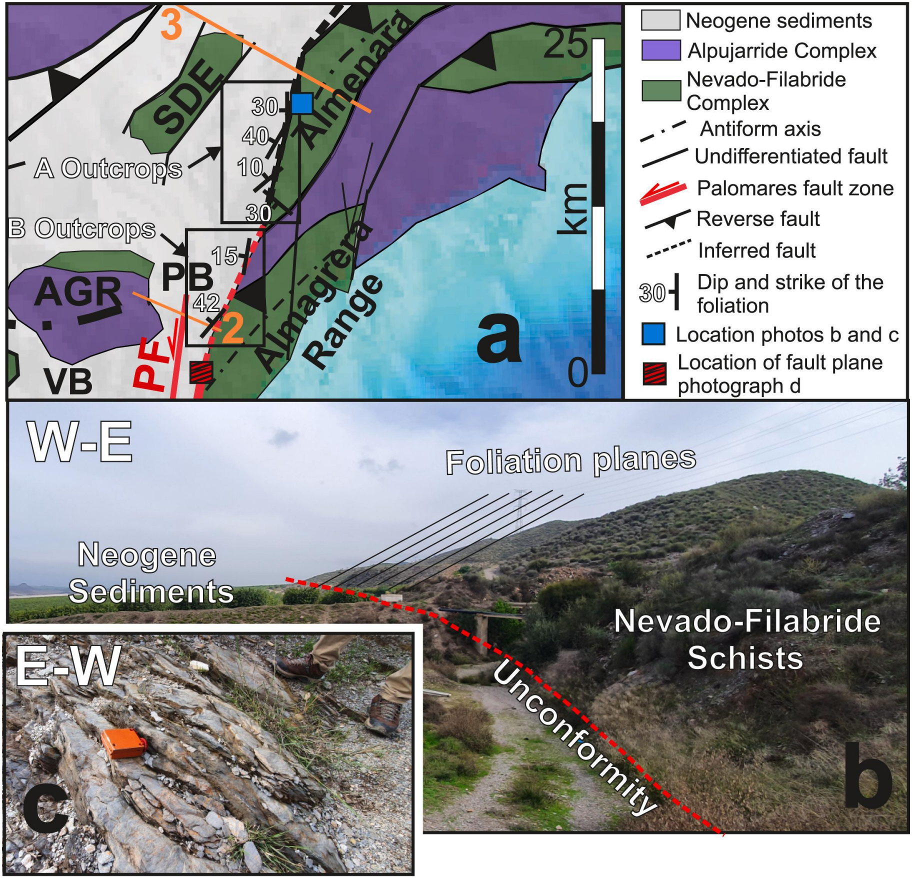

3
SDE
Almenara
25
A Outcrops
30
40
10
30
B Outcrops
15
PB
AGR
42
2
Almagrera
Range
a
km
0
VB
PF
Neogene sediments
Alpujarride Complex
Nevado-Filabride Complex
Antiform axis
Undifferentiated fault
Palomares fault zone
Reverse fault
Inferred fault
30 Dip and strike of the foliation
Location photos b and c
Location of fault plane photograph d
W-E
Foliation planes
Neogene Sediments
Nevado-Filabride Schists
Unconformity
b
E-W
c

Figure 6

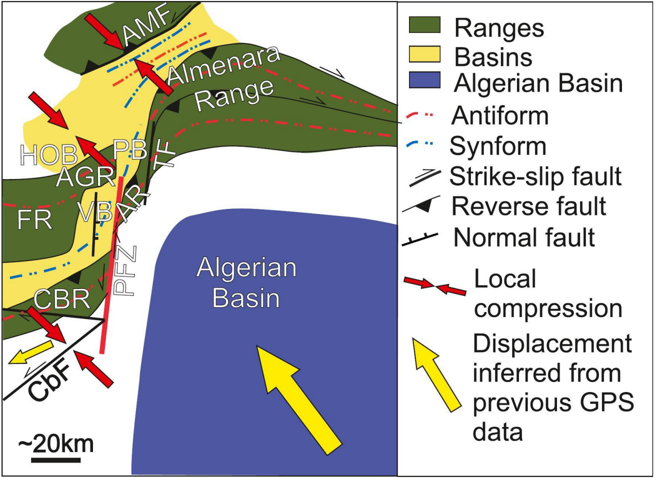
AMF
Almenara
Range
HOB
PB
AGR
TF
FR
VB
AR
PFZ
CBR
CbF
Algerian
Basin
~20km
Ranges
Basins
Algerian Basin
Antiform
Synform
Strike-slip fault
Reverse fault
Normal fault
Local
compression
Displacement
inferred from
previous GPS
data

Figure 7